

Accepted Manuscript

The azatryptophan-based fluorescent platform for *in vitro* rapid screening of inhibitors disrupting IKK β -NEMO interaction

Wei-Chih Chao, Tzu-Hsuan Chiang, Prakash D. Chaudhari, Li-Ju Lin, Jyh-Feng Lu, Bor-Cherng Hong, Jinn-Shyan Wang, Ta-Chun Lin, Jiun-Yi Shen, Pi-Tai Chou

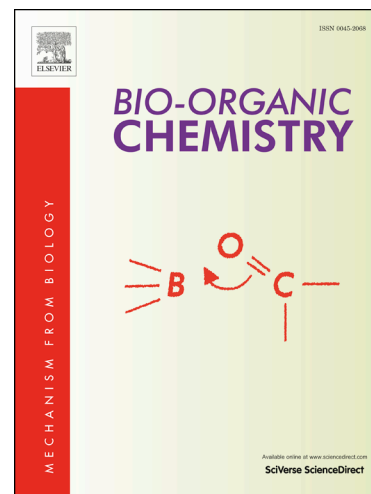
PII: S0045-2068(18)30809-5
DOI: <https://doi.org/10.1016/j.bioorg.2018.09.006>
Reference: YBIOO 2503

To appear in: *Bioorganic Chemistry*

Received Date: 2 August 2018
Revised Date: 4 September 2018
Accepted Date: 6 September 2018

Please cite this article as: W-C. Chao, T-H. Chiang, P.D. Chaudhari, L-J. Lin, J-F. Lu, B-C. Hong, J-S. Wang, T-C. Lin, J-Y. Shen, P-T. Chou, The azatryptophan-based fluorescent platform for *in vitro* rapid screening of inhibitors disrupting IKK β -NEMO interaction, *Bioorganic Chemistry* (2018), doi: <https://doi.org/10.1016/j.bioorg.2018.09.006>

This is a PDF file of an unedited manuscript that has been accepted for publication. As a service to our customers we are providing this early version of the manuscript. The manuscript will undergo copyediting, typesetting, and review of the resulting proof before it is published in its final form. Please note that during the production process errors may be discovered which could affect the content, and all legal disclaimers that apply to the journal pertain.



The azatryptophan-based fluorescent platform for *in vitro* rapid screening of inhibitors disrupting IKK β -NEMO interaction

Wei-Chih Chao,^a Tzu-Hsuan Chiang,^{a,b} Prakash D. Chaudhari,^c Li-Ju Lin,^{a,b} Jyh-Feng Lu,^{*b} Bor-Cherng Hong,^{*c} Jinn-Shyan Wang,^{*b} Ta-Chun Lin,^a Jiun-Yi Shen,^a Pi-Tai Chou^{*a}

^a Department of Chemistry and Center for Emerging Material and Advanced Devices, National Taiwan University, Taipei, Taiwan. E-mail: chop@ntu.edu.tw

^b School of Medicine, Fu Jen Catholic University, New Taipei City, Taiwan. E-mail: 049696@mail.fju.edu.tw; 034407@mail.fju.edu.tw

^c Department of Chemistry and Biochemistry, National Chung Cheng University, Chia-Yi, Taiwan. E-mail: chebch@ccu.edu.tw

Abstract

The nuclear factor- κ B (NF- κ B) plays an important role in inflammatory and immune responses. Aberrant NF- κ B signaling is implicated in multiple disorders, including cancer. Targeting the regulatory scaffold subunit I κ B kinase γ (IKK γ /NEMO) as therapeutic interventions could be promising due to its specific involvement in canonical NF- κ B activation without interfering with non-canonical signaling. In this study, the use of unnatural amino acid substituted IKK β with unique photophysical activity to sense water environment changes upon interaction with NEMO provides a powerful *in vitro* screening platform that would greatly facilitate the identification of compounds having the potential to disrupt IKK β -NEMO interaction, and thus specifically modulate the canonical NF- κ B pathway. We then utilized a competitive

binding platform to screen the binding ability of a number of potential molecules being synthesized. Our results suggest that a lead compound (-)-PDC-099 is a potent agent with ascertained potency to disrupt IKK β -NEMO complex for modulating NF- κ B canonical pathway.

Introduction

The nuclear factor- κ B (NF- κ B) signal transduction pathway regulates a variety of important mammalian biological functions, including immune and inflammatory responses, differentiation, cell growth, tumorigenesis, and apoptosis.[1, 2] Inhibition of the NF- κ B signaling provides therapeutic potential for arthritis, asthma, autoimmune diseases, and certain cancers that involve NF- κ B hyperactivation.[3, 4] Moreover, inhibition of the cancer cell-specific signaling of NF- κ B with oncogenic functions offers an attractive alternative therapeutic target for malignancies.[5-9]

The pathways of NF- κ B activation are broadly classified as the canonical (or classical) pathway and the non-canonical (or alternative) pathway, depending upon the nature of the I κ B proteins and I κ B kinase (IKK) complexes involved. The IKK complex typically consists of two homologous catalytic subunits IKK α and IKK β , and a regulatory scaffold subunit IKK γ (also known as NEMO).[10-12] The regulatory subunit NEMO serves as a critical integrating platform that couples upstream receptor signaling complexes to the catalytic IKKs.[2, 13] In the canonical NF- κ B pathway,

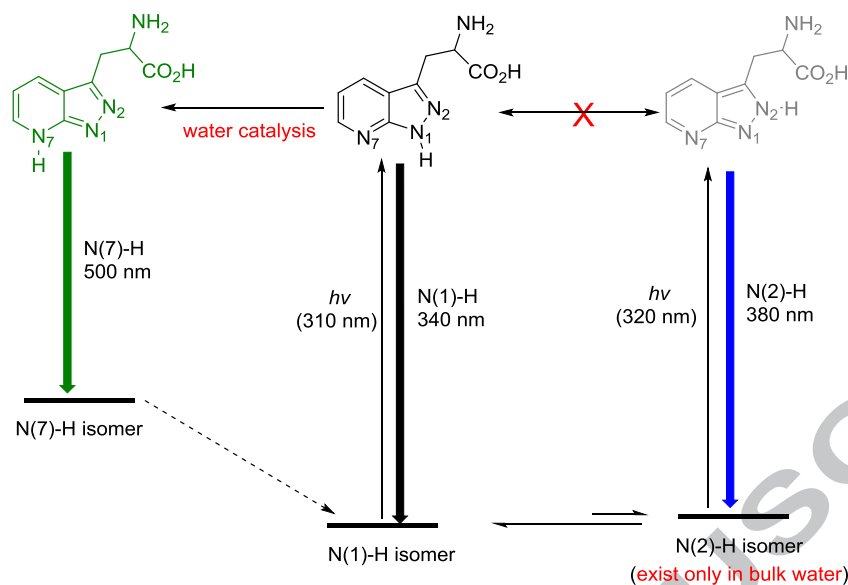
exposure to inflammatory cytokines or other immune signals leads to the rapid activation of the IKK complex. Alternatively, the non-canonical NF- κ B pathway is induced by a distinct group of tumor necrosis factor (TNF)-family ligands,[14, 15] and governs normal developmental and immune processes.[16-18] In contrast to canonical NF- κ B signaling, which is subject to rapid and transient activation, the non-canonical NF- κ B pathway is activated with distinctively slower kinetics. Additionally, the non-canonical pathway neither requires IKK β or IKK γ /NEMO nor involves the proteolysis of canonical I κ Bs. It exclusively relies on IKK α and the signal-induced processing of p100 to release RelB/p52 heterodimers.[10, 14, 19]

Due to the pleiotropic and ubiquitous functions of NF- κ B, a challenge with conventional utilization of NF- κ B or IKK β inhibitors as anti-tumor agents is to achieve cancer cell specificity.[20] Agents that target these effectors with functional restriction to cancer cells and lack toxicities of global NF- κ B could provide safer and selective anti-cancer therapies. Accordingly, targeting the regulatory scaffold subunit IKK γ (NEMO) as therapeutic interventions could be promising due to its specific involvement in canonical NF- κ B activation without interfering with non-canonical signaling. The interaction of IKK β with NEMO has previously been studied by measuring the effects of IKK β mutagenesis using a qualitative pull-down assay, and by measuring the binding activity of IKK β -derived peptides of various lengths.[21]

These reports established that NEMO interacted with the C-terminal region of IKK β encompassing residues 701–745. Residues 737–742 of IKK β (738–743 for IKK α) have been shown to comprise a critical motif for binding NEMO, which is also known as the “NEMO binding domain” (NBD), [22, 23] is conserved in IKK α and IKK β . The 11-mer IKK β peptide (residues 735–745) encompassing the NBD was shown to block the interaction of IKK β with recombinant GST-NEMO and to disrupt the preformed NEMO/IKK β complexes. [23] NBD-containing IKK β peptides have also been shown to inhibit NEMO/IKK β binding and NF- κ B signaling and function in cells and in animals. [22, 24, 25]

Mutagenesis of two highly conserved tryptophan (Trp) residues of IKK β , Trp739 and Trp741, to alanine, resulting in the loss of NEMO binding activity in a pull-down assay, suggested their critical role in the binding of IKK β to NEMO. [23] Mutation of either W739F or W741F maintained NEMO binding; however, mutation of W741Y, but not W739Y, blocked association with NEMO. [23] It was suggested that the hydroxyl side chain of Y739 might form an additional intramolecular hydrogen bond with the backbone carbonyl of F734 and maintained the native IKK β conformation. In contrast, Y741 might not have an appropriate hydrogen-bonding counterpart, which caused a desolvation upon burial in the nonpolar NEMO cavity, resulting in destabilizing the IKK β conformation and hence a reduction in NEMO binding. [26]

In yet another approach, a Trp analogue 7-azatryptophan ((7-aza)Trp) is a powerful sensor in probing the local polarity. Upon electronic excitation (7-aza)Trp undergoes intramolecular charge transfer from pyrrolic (highest occupied molecular orbital, HOMO) to pyridyl (lowest unoccupied molecular orbital, LUMO) moiety. As a result, the emission is strongly affected by the polarity of the environment, being red shifted from 320 nm in nonpolar solvent to ~400 nm in water.[27, 28] Recently, by the use of 2,7-diazatryptophan ((2,7-aza)Trp) (see Scheme 1) to replace Trp, a more direct method in sensing water molecules has been reported and evaluated for their possible functionality in proteins.[29-31] Unlike (7-aza)Trp, the emission of (2,7-aza)Trp is not sensitive to the environment polarity. Instead, (2,7-aza)Trp exists predominantly as the N(1)-H isomer with a minor N(2)-H isomer in neutral aqueous solution, in which the N(1)-H isomer, upon excitation, undergoes water molecules catalyzed proton transfer, giving both 340 nm (N(1)-H) and 500 nm (N(7)-H) emission. The N(2)-H isomer with ~380 nm emission only exists in bulk water and generally disappears in protein where (2,7-aza)Trp is microsolvated by water molecules (see Scheme 1). Thus, the multiple emission of (2,7-aza)Trp has been proved to be ideal for probing water environment surrounding Trp in protein.[29-31]



Scheme 1. The ground-state equilibrium between N(1)-H and N(2)-H for (2,7-aza)Trp in neutral water and water catalyzed N(1)-H→N(7)-H proton transfer in the excited state.

In this study, (7-aza)Trp and (2,7-aza)Trp were applied to replace Trp739 or Trp741 of the NBD-containing IKK β peptide, the combination of which then acted as a fluorescence sensor for sensing polarity, proximal and relayed water molecules around the binding interface of IKK β -NEMO. We further utilized the characteristic N(2)-H isomer of (2,7-aza)Trp existing only in bulk water to develop a fluorescent platform for in vitro rapid screening of inhibitors disrupting IKK α/β -NEMO interaction.

Knowing that Trp739 and Trp741 play an important role in IKK β -NEMO binding process, in this platform, we made attempts to screen a number of spirocyclic oxindole derivatives that have potential to bind Trp in an aim to search for the lead

molecules. Recent anticancer progress has shown spiro-oxindole derivatives as potent small molecule inhibitors of the p53-MDM2 interaction, in which the spiro core structure emerged as the starting point, so that the oxindole ring inserts into the binding cavity occupied by Trp23 indole in p53.[32] We also intended to investigate the enantiomer dependent activities of spirocyclic oxindoles derivatives. Investigation of biological activities of the natural and synthetic derivatives revealed that (-)-enantiomers of notoamides A and B, 6-epi-notoamide T, and stephacidin A inhibited receptor activator of NF- κ B ligand (RANKL)-induced osteoclastogenic differentiation of murine RAW264 cells more strongly than their respective (+)-enantiomers.[33] As a result, among a number of spirocyclic oxindoles derivatives being synthesized our results suggest that a lead compound (-)-PDC-099 is a potent agent for modulating NF- κ B canonical pathway. Detail of the results, discussion and perspectives is elaborated as follows.

Results and Discussions

Polarity and water environment of Trp439 and Trp441 in IKK β ₇₃₅₋₇₄₅

The fluorescence spectral changes were used to investigate the NEMO binding with synthetic peptides (7-aza)Trp-IKK β ₇₃₅₋₇₄₅ and (2,7-aza)Trp-IKK β ₇₃₅₋₇₄₅. Similar to that of 7-azaindole,[34, 35] the fluorescence of (7-aza)Trp has been reported to undergo an

excited-state charge transfer from the pyrrolic to the pyridyl moiety and hence exhibit the polarity-dependent emission peak wavelength, namely the emission solvatochromism.[35] As shown in Figure 1, in the absence of NEMO, upon 310 nm excitation where only (7-aza)Trp in (7-aza)Trp-IKK β ₇₃₅₋₇₄₅ is excited, the emission of (7-aza)Trp-IKK β ₇₃₅₋₇₄₅ maximized at 394, 396 and 392 nm for (7-aza)Trp739/741-IKK β ₇₃₅₋₇₄₅, (7-aza)Trp739-IKK β ₇₃₅₋₇₄₅ and (7-aza)Trp741-IKK β ₇₃₅₋₇₄₅, respectively, indicating that environment of Trp741 is more non-polar than that of Trp739. Upon binding with NEMO, each original emission peak gradually blue shifted to 385, 381 and 387 nm, respectively, showing the change in polarity to a less polar environment around the (7-aza)Trp residue in three peptides. It is noteworthy that (7-aza)Trp741-IKK β ₇₃₅₋₇₄₅ has less shift of the emission peak wavelength (i.e. less polarity changes) than that of (7-aza)Trp739-IKK β ₇₃₅₋₇₄₅, suggesting that the environment of Trp739-IKK β ₇₃₅₋₇₄₅ binding site in NEMO was more hydrophobic. Previous research indicated potential hydrophobic interaction between Trp739 (in IKK β) and Phe97 (in NEMO) as well as between Trp741 (in IKK β) and Ala100 or Arg101 (in NEMO).[26] The larger polarity change upon binding of (7-aza)Trp739-IKK β ₇₃₅₋₇₄₅ with NEMO suggests that the hydrophobic interaction of Phe97:Trp739 (NEMO:IKK β) is much stronger than that of Ala100/Arg101:Trp741.

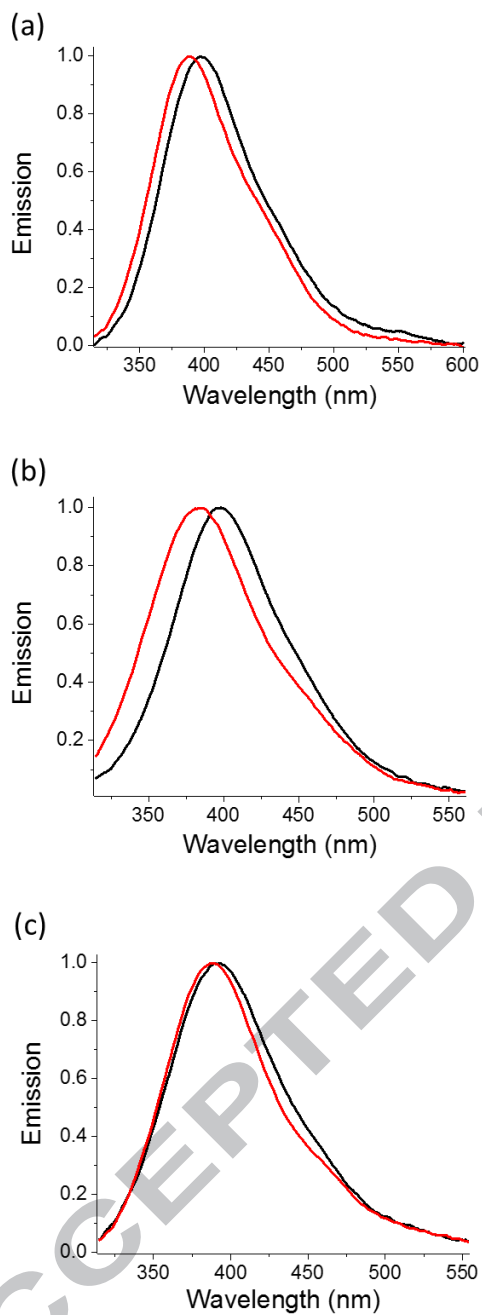


Figure 1. Normalized emission spectra of 1 μM (a) (7-aza)Trp739/741-IKK $\beta_{735-745}$, (b)

(7-aza)Trp739-IKK $\beta_{735-745}$ and (c) (7-aza)Trp741-IKK $\beta_{735-745}$ before (black line) and

after (red line) binding with 4 μM NEMO. The excitation wavelength (λ_{ex}) is 310 nm.

Similar to that of free (2,7-aza)Trp in aqueous solution (see Scheme 1),[29] multiple

emission bands were observed for (2,7-aza)Trp-IKK β ₇₃₅₋₇₄₅ in neutral buffer, consisting of the N(1)-H isomer emission (340 nm), N(2)-H emission (380 nm) and N(7)-H emission (500 nm) (Figure 2a-2c). Dramatic changes in spectral features were observed during the titration of (2,7-aza)Trp-IKK β ₇₃₅₋₇₄₅ with NEMO, in which the N(2)-H (380 nm) and N(7)-H (500 nm) emission bands gradually decreased, accompanied by the increase of the N(1)-H emission at 340 nm. At the end of the titration, only the N(1)-H 340 nm emission was observed. The apparent spectral changes during titration are due to the loss of bulk water surrounding (2,7-aza)Trp-IKK β ₇₃₅₋₇₄₅ upon (2,7-aza)Trp-IKK β ₇₃₅₋₇₄₅/NEMO binding, leading to the lack of the N(2)-H population. As shown in Figure 2d-2f, among (2,7-aza)Trp739/741-IKK β ₇₃₅₋₇₄₅, (2,7-aza)Trp739-IKK β ₇₃₅₋₇₄₅ and (2,7-aza)Trp741-IKK β ₇₃₅₋₇₄₅, the N(2)-H 380 nm emission of (2,7-aza)Trp741-IKK β ₇₃₅₋₇₄₅ reveals the largest decrease in intensity, inferring the most significant change of its surrounding from water-rich to water-scant environment. The result implies that (2,7-aza)Trp741-IKK β ₇₃₅₋₇₄₅ may serve as an ideal probe in a competition assay for screening small molecule drugs interfering the binding of IKK β ₇₃₅₋₇₄₅ with NEMO, as elaborated in the following section.

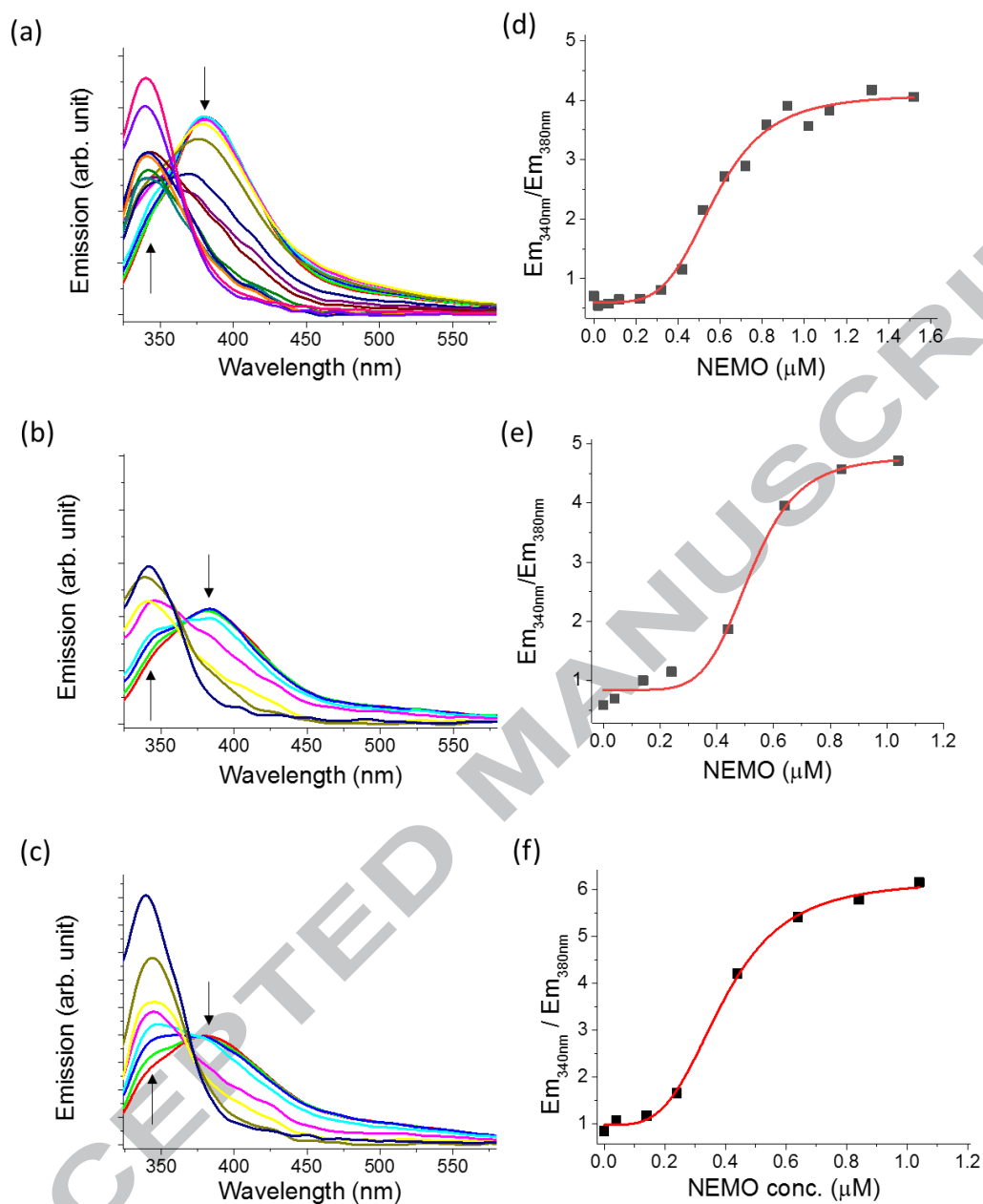


Figure 2. Emission spectra of (2,7-aza)Trp -IKK $\beta_{735-745}$ titrated with NEMO. Spectra of 1 μ M (a) (2,7-aza)Trp739/741-IKK $\beta_{735-745}$, (b) (2,7-aza)Trp739-IKK $\beta_{735-745}$ and (c) (2,7-aza)Trp741-IKK $\beta_{735-745}$ binding with increasing concentrations of NEMO (as indicated by arrows). The excitation wavelength (λ_{ex}) is 310 nm. Each dissociation constants (Kd) were determined by fitting curve of Em_{340nm}/Em_{380nm} versus NEMO concentration as 0.58, 0.52 and 0.42 μ M for (d) (2,7-aza)Trp739/741-IKK $\beta_{735-745}$

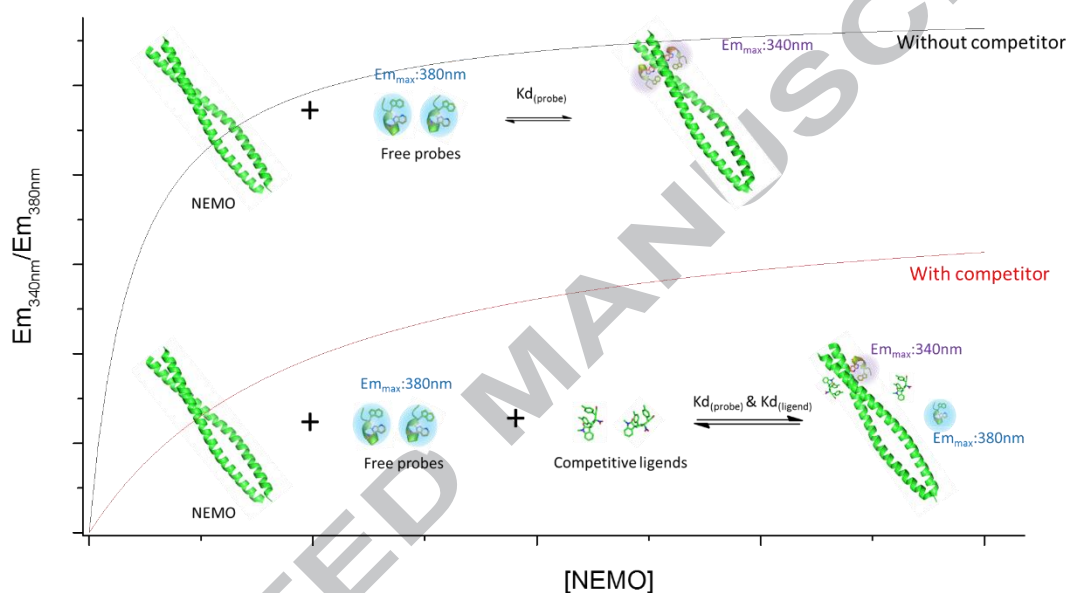
(R-square = 0.988), (e) (2,7-aza)Trp739-IKK β ₇₃₅₋₇₄₅ (R-square = 0.983) and (f) (2,7-aza)Trp741-IKK β ₇₃₅₋₇₄₅ (R-square = 0.996), respectively.

Effects of potential inhibitors on the binding of IKK β ₇₃₅₋₇₄₅ with NEMO

As for the control, during the binding of NEMO with (2,7-aza)Trp741-IKK β ₇₃₅₋₇₄₅, the decrease of the N(2)-H (380 nm) emission and the increase of N(1)-H (340 nm) emission were clearly observed, therefore, the sum of the emission differences at 340 nm and 380 nm can be used to represent the binding state. The concentration of 1 μ M (2,7-aza)Trp741-IKK β ₇₃₅₋₇₄₅ was used for monitoring the emission intensity at 340 and 380 nm upon binding with NEMO as well as in the competing assay. By fitting the plot of Em_{340nm}/Em_{380nm} intensity ratio versus NEMO concentration (see Figure 2c and see eq. S1 in SI), the dissociation constant (K_d) for (2,7-aza)Trp741-IKK β ₇₃₅₋₇₄₅ was determined to be 0.42 μ M.

To investigate inhibitors on the binding of IKK β ₇₃₅₋₇₄₅ with NEMO, the canonical IKK β ₇₃₅₋₇₄₅ peptide was selected as a binding reference to establish the competition assay, in which 1 μ M canonical IKK β ₇₃₅₋₇₄₅ peptide was mixed with 1 μ M (2,7-aza)Trp741-IKK β ₇₃₅₋₇₄₅ peptide and titrated with increasing concentration of NEMO. Binding curves were then fitted to a formula describing competitive binding of two different ligands to the same site on a protein (see Scheme 2 and eq. S1 in SI).

As shown in Table 1, the canonical amino acid IKK β ₇₃₅₋₇₄₅ gave a similar K_d value ($0.46 \pm 0.05 \mu\text{M}$) to (2,7-aza)Trp741-IKK β ₇₃₅₋₇₄₅ ($0.42 \pm 0.02 \mu\text{M}$), indicating that replacement of (2,7-aza)Trp in IKK β ₇₃₅₋₇₄₅ did not influence its binding ability with NEMO.



Scheme 2. Schematic presentation of competitive binding experiments to fit the dissociation constant of samples.

We first synthesized a series of phenothiazine and phenoxazine derivatives from N-ethylphenothiazine (CP1 to CP7, structure shown in SI). Phenothiazine and phenoxazine derivatives, such as CP1, have been reported to have potential to interfere the binding of IKK β with NEMO.[36] Screening was carried out by evaluating K_d values of phenothiazine and phenoxazine derivatives upon competing

with (2,7-aza)Trp741-IKK β ₇₃₅₋₇₄₅ binding to NEMO. Even though the N-ethylphenothiazine (CP1, Scheme 3) has the lowest K_d ($0.63 \pm 0.05 \mu\text{M}$) among all screened phenothiazine and phenoxazine derivatives, the K_d value is still slightly higher than that of the canonical IKK β ₇₃₅₋₇₄₅ peptide ($0.46 \pm 0.05 \mu\text{M}$). Furthermore, the phenoxazine derivatives showed higher K_d than phenothiazine derivatives, indicating that the thiazine group is more likely to interfere IKK β ₇₃₅₋₇₄₅-NEMO binding than the oxazine group. As a result, these seven phenothiazines and phenoxazine derivatives did not provide satisfactory efficacy to alter IKK β ₇₃₅₋₇₄₅-NEMO binding.

Other series of potential compounds, including polysubstituted spirocyclic oxindoles (vide supra, see Scheme 3 and SI for corresponding structures,) such as 3-allylindolin-2-one derivatives,[37] were then synthesized and their K_d was determined by competing with (2,7-aza)Trp741-IKK β ₇₃₅₋₇₄₅ and NEMO binding. Pertinent data are listed in Table 1. As shown in Table 1, although (-)-PDC-098 and (-)-PDC-100 are only different in the substitution of two -CH₃ groups with Br atoms, (-)-PDC-098 shows a significantly lower K_d (see Table 1), indicating the importance of increasing affinity via hydrophobic interaction rather than the sizes of the sidechains. Also, K_d of both (-) optical isomers are lower than that of (+) isomers of PDC-099 and PDC-100, manifesting the chirality effect. The results clearly indicate

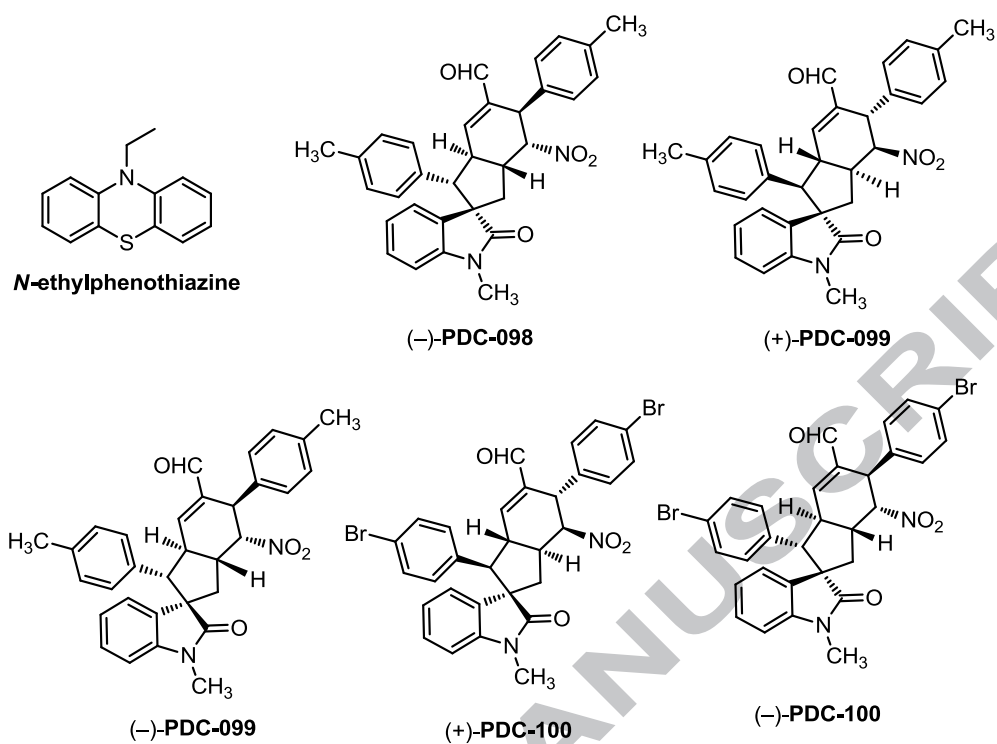
that the 3D geometric structure is crucial for their ability to influence the IKK β ₇₃₅₋₇₄₅-NEMO binding. In our screening study, it is noteworthy that (-)-PDC-099 is the most potent inhibitor for IKK β ₇₃₅₋₇₄₅-NEMO binding, which exhibits a K_d value with SD (n=3) as low as $0.08 \pm 0.01 \mu\text{M}$ (Figure 3). We also performed surface plasmon resonance (SPR) assay to validate direct interaction between (-)-PDC-099 and NEMO. The equilibrium dissociation constant K_d between (-)-PDC-099 and NEMO was around $0.099 \mu\text{M}$ (Figure S24), which matches well with that obtained from our fluorescence assay.

To explore the possible interactions between the inhibitor and NEMO, the computational docking approach has been performed. Figure 4 shows the docking of (-)-PDC-099 and (+)-PDC-099 into the NEMO receptor cavity. The CDOKCER interaction energy indicates there is a more favorable interaction between the (-)-PDC-099 and NEMO (-35.02 kcal/mole) than the interaction between the (+)-PDC-099 and NEMO (-29.04 kcal/mole). (-)-PDC-099 was predicted to bind to the NEMO specific pockets via a hydrogen bond to K96 and hydrophobic contacts with F92, L93 and A100 residues of chain B, as well as F97, A100 and V104 residues of chain D, in which chains B and D were defined by NEMO/IKK β association domain structure (PDB: 3BRV). In stark contrast, (+)-PDC-099 bind to the NEMO specific pockets via hydrophobic contacts with L93 and A100 residues of chain B as

well as M95, F97 and A100 residues of chain D. The additional hydrogen bonding to K96 and better geometric matching rationalize higher binding affinity of (-)-PDC-099 than that of (+)-PDC-099 to NEMO.

Table 1. The dissociation constant (K_d) for the binding of $\text{IKK}\beta_{735-745}$ and screened compounds with NEMO ($n = 3$; \pm SD) as determined by competing with (2,7-aza)Trp741- $\text{IKK}\beta_{735-745}$.

Sample	K_d (μM)	Sample	K_d (μM)
(2,7-aza)Trp741- $\text{IKK}\beta_{735-745}$	0.42 ± 0.02	(\pm)-PDC-091	0.67 ± 0.04
$\text{IKK}\beta_{735-745}$	0.46 ± 0.05	(\pm)-PDC-092	0.79 ± 0.03
N-ethylphenothiazine (CP1)	0.63 ± 0.05	(\pm)-PDC-111	2.58 ± 0.12
CP2	1.33 ± 0.07	(-)-PDC-095	0.60 ± 0.05
CP3	0.95 ± 0.05	(-)-PDC-098	0.19 ± 0.02
CP4	0.73 ± 0.05	(-)-PDC-099	0.08 ± 0.01
CP5	4.88 ± 0.19	(+)-PDC-099	0.53 ± 0.05
CP6	1.60 ± 0.06	(-)-PDC-100	0.42 ± 0.03
CP7	1.97 ± 0.05	(+)-PDC-100	1.38 ± 0.08



Scheme 3. Chemical structures of N-ethylphenothiazine and polysubstituted spirocyclic oxindoles derivatives.

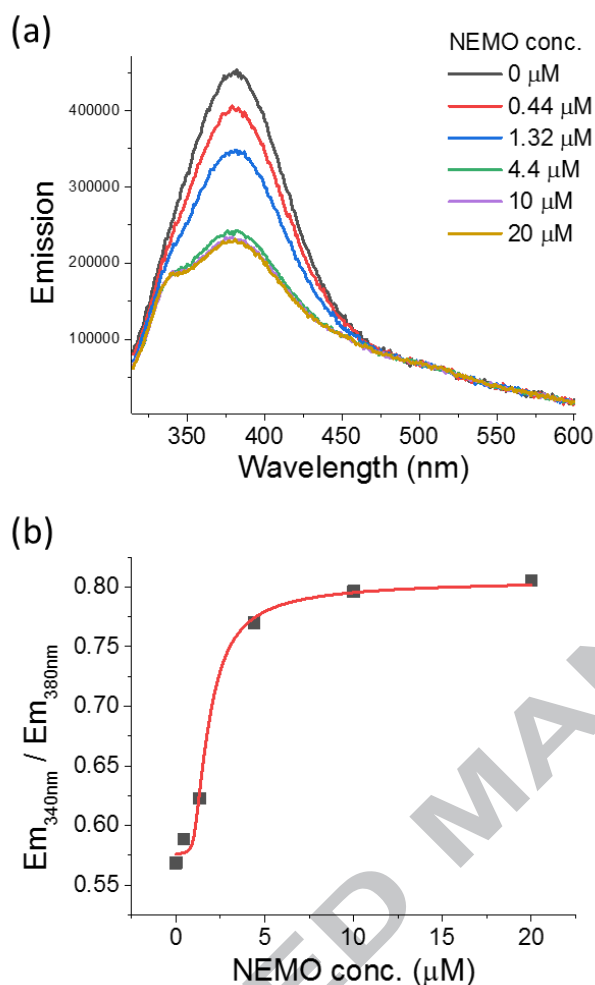


Figure 3. (a) Emission spectra of 1 μM (-)-PDC-099 and 1 μM (2,7-aza)Trp741-IKKβ₇₃₅₋₇₄₅ mixture titrated with NEMO. The excitation wavelength (λ_{ex}) is 310 nm. (b) The dissociation constant (Kd) for (-)-PDC-099 were then determined by fitting the competition curve (R-square = 0.986) of Em_{340nm}/Em_{380nm} versus NEMO concentration.

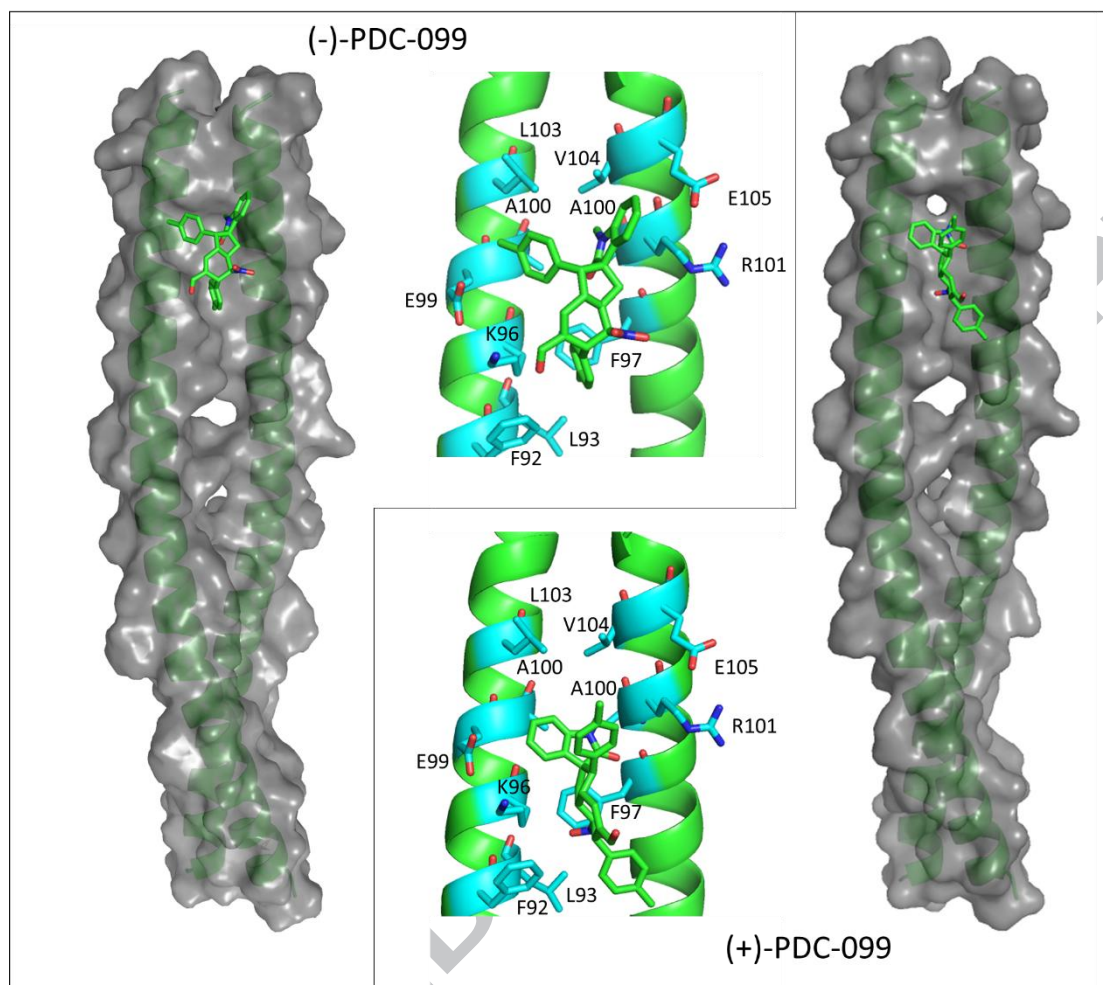


Figure 4. The predicted docking of (-)-PDC-099 and (+)-PDC-099 into the NEMO receptor cavity formed by α -helix chains B and D based on NEMO/IKK β association domain structure (PDB: 3BRV).

Conclusion

In summary, we used unnatural amino acid substituted IKK β ₇₃₅₋₇₄₅ peptides to act as fluorescent probes for sensing polarity, proximal and relayed water molecules around the binding interface of IKK β -NEMO. By particular characteristic of N(2)-H isomer for (2,7-aza)Trp that only exists in bulk water, we establish a novel and facile

methodology to screen ideal organic molecules for inhibiting IKK β -NEMO complex formation. Aiming at targeting NEMO in cancer cells, the therapeutic interventions specifically inhibit canonical NF- κ B activation can be achieved without interfering with non-canonical NF- κ B signaling. Conclusively, among a number of potential molecules being synthesized, our results suggest that (-)-PDC-099 is a potent agent with ascertained potent to disrupt IKK β -NEMO complex for modulating NF- κ B canonical pathway. The development of a simple, cost-effective and highly specific *in vitro* screening platform would greatly facilitate the identification of compounds that specifically modulate the canonical NF- κ B pathway by targeting IKK β -NEMO interaction.

Experimental section

Protein expression and purification

DNA encoding the full-length NEMO₁₋₄₁₉ was obtained by PCR using cDNA template derived from human leukocytes. NEMO expression vectors were generated by sub-cloning NEMO-encoding DNA fragments into a P_{tac} promoter driven pCW plasmid under inducible regulation by lacI. The resulting NEMO cDNAs were transformed into BL21 based *Escherichia coli* strain C43 for protein expression. Bacterial cultures were grown at 37 °C in LB medium containing 100 μ g/ml

ampicillin to an OD₆₀₀ of 0.6-0.8. Expression of the protein was induced with 1 mM IPTG and the bacteria were further cultured at 30 °C for 18-20hr. The cells were harvested by centrifugation at 4 °C, 5000 rpm, for 15 minutes. The pellet was resuspended in lysis buffer (50 mM NaPi, pH 7.5, containing 100 mM NaCl, 2 mM MgCl₂, 10% glycerol), and incubated with 1 mg/ml lysozyme and 10 µg/mL DNase for 20 minutes. Then the final concentration of 4M urea and 0.05% β-mercaptoethanol were added and stirred at room temperature for overnight. After sonication, the lysate was centrifuged at 30,000 for 1 hour at 4 °C and the supernatant was mixed with Ni-NTA resin (Qiagen, GmbH, Germany), which was pre-equilibrated with denaturing buffer (50 mM NaPi, pH 7.8, containing 4 M Urea and 300 mM NaCl), for binding overnight at room temperature. The bound Ni-NTA resin was packed in the column and washed with denaturing buffer. Then washed with native wash buffer (50 mM NaPi, pH 7.5, containing 300 mM NaCl) and followed by the same solution with 2 mM Histidine (His). The recombinant NEMO protein was eluted with native elution buffer (50 mM NaPi, pH 7.5, containing 300 mM NaCl and 200 mM His). Protein concentration was quantitatively determined with Bradford protein assay and adjust to 50 µM before stored at -80 °C.

Synthesis of IKKβ₇₃₅₋₇₄₅ peptides

The IKKβ₇₃₅₋₇₄₅ peptides with or without unnatural amino acid replacement were

synthesized and purified to greater than 95% homogeneity by Scientific Biotech Corp.

(Taipei Taiwan R.O.C.).

General Procedure for the Synthesis of Polysubstituted Spirocyclic Oxindoles.[37]

To a solution of (*S*)- α,α -bis[3,5-bis(trifluoromethyl)phenyl]-2-pyrrolidinemethanol trimethylsilyl ether (Jørgensen–Hayashi catalyst, 15.4 mg, 0.026 mmol, 0.2 equiv) and (*E*)-3-(*p*-tolyl)acrylaldehyde (42.7 mg, 0.32 mmol, 2.5 equiv) in toluene (0.26 mL) was added (*E*)-1-methyl-3-(3-nitroallyl)indolin-2-one (30.0 mg, 0.13 mmol, 1.0 equiv). The resulting solution was stirred at 45 °C for 92 h until the completion of the reaction, as monitored by TLC. The resulting mixture was diluted with EtOAc (10 mL), washed with water (5 mL) and brine (5 mL), dried over MgSO₄, and concentrated *in vacuo* to give the crude residue. The diastereomeric ratio, as determined by ¹H NMR analysis of the crude mixture, was found to be 72/28. The residue was purified by flash column chromatography with 10% EtOAc–hexane (*R_f* = 0.57 for (–)-**PDC-098**, *R_f* = 0.52 for (–)-**PDC-099**, developed twice in 30% EtOAc–hexane) to give the product (–)-**PDC-098** and (–)-**PDC-099** (40.6 mg, 62 % combined yield).

Selected data for (–)-**PDC-098**: white solid, m.p. 144–146 °C; [α]_D²⁶ –42.8 (*c* 1, CHCl₃); IR (neat): 3020, 2924, 2857, 1691, 1612, 1546, 1513, 1493, 1470, 1375, 1355, 1309, 1266, 1142, 1086, 1024, 820, 753 cm⁻¹; ¹H NMR (500 MHz, CDCl₃):

δ 9.40 (s, 1 H), 7.27 – 7.21 (m, 2 H), 7.19 (d, $J = 8.0$ Hz, 2 H), 7.12 – 7.05 (m, 3 H), 7.04 (s, 1 H), 6.96 (d, $J = 8$ Hz, 2 H), 6.72 (d, $J = 8.0$ Hz, 2 H), 6.61 (d, $J = 8.0$ Hz, 1 H), 4.94 (d, $J = 3.0$ Hz, 1 H), 4.65 (s, 1 H), 3.71 (t, $J = 12.5$ Hz, 1 H), 3.27 (d, $J = 12.5$ Hz, 1H), 2.74 – 2.64 (m, 1 H), 2.70 (m, 3 H), 2.41 (t, $J = 13.5$ Hz, 1 H), 2.35 (s, 3 H), 2.25 (s, 3 H), 2.10 (dd, $J = 13.0, 8.0$ Hz, 1 H); ^{13}C NMR (125 MHz, CDCl_3): δ 192.0 (CH), 178.0 (C), 149.2 (CH), 143.6 (C), 141.2 (C), 137.6 (C), 137.4 (C), 136.5 (C), 133.5 (C), 130.9 (C), 130.0 (two CH), 128.9 (two CH), 128.3 (CH), 127.9 (two CH), 127.8 (two CH), 122.7 (CH), 122.0 (CH), 107.8 (CH), 87.9 (CH), 59.4 (CH), 57.1 (C), 44.0 (CH), 40.7 (CH), 40.3 (CH), 34.7 (CH_2), 25.7 (CH_3), 21.04 (CH_3), 21.02 (CH_3); MS (m/z , relative intensity): 507 ($\text{M}^+ + 1$, 4), 506 (M^+ , 13), 460 (54), 442 (5), 368 (14), 317 (13), 301 (11), 271 (12), 262 (11), 241 (15), 209 (18), 184 (20), 160 (100), 147 (55), 130 (26), 105 (45); exact mass calculated for $\text{C}_{32}\text{H}_{30}\text{N}_2\text{O}_4$ (M^+): 506.2206; found: 506.2204.

Selected data for (–)-**PDC-099**: white solid, m.p. 86–88 °C; $[\alpha]_{\text{D}}^{26} -26.6$ (c 1, CHCl_3); ^1H NMR (500 MHz, CDCl_3): δ 9.40 (s, 1 H), 7.17 (d, $J = 8.0$ Hz, 2 H), 7.08 (d, $J = 8.0$ Hz, 2 H), 7.06 – 7.01 (m, 2 H), 6.96 (d, $J = 7.0$ Hz, 1 H), 6.90 – 6.84 (m, 3 H), 6.79 (d, $J = 8.0$ Hz, 2 H), 6.52 (d, $J = 8.0$ Hz, 1 H), 4.93 (d, $J = 3.0$ Hz, 1 H), 4.66 (s, 1 H), 3.63 (d, $J = 13.0$ Hz, 1 H), 3.34 (t, $J = 12.5$ Hz, 1 H), 3.11 (s, 3 H), 2.91 – 2.83 (m, 1 H), 2.37 (dd, $J = 13.5, 8.0$ Hz, 1 H), 2.32 (s, 3 H), 2.17 (s, 3 H), 2.07 (dd, J

= 13.5, 11.4 Hz, 1 H); ^{13}C NMR (125 MHz, CDCl_3): δ 191.9 (CH), 180.4 (C), 148.6 (CH), 142.7 (C), 141.5 (C), 137.7 (C), 137.0 (C), 135.9 (C), 132.1 (C), 131.7 (C), 130.0 (two CH), 128.8 (two CH), 127.93 (CH), 127.89 (two CH), 127.7 (two CH), 124.2 (CH), 122.4 (CH), 107.7 (CH), 88.2 (CH), 57.30 (C), 57.26 (CH), 44.1 (CH), 42.0 (CH), 39.4 (CH), 35.8 (CH_2), 26.3 (CH_3), 21.01 (CH_3), 20.95 (CH_3).

(+)-**PDC-098** and (+)-**PDC-099** were prepared by the same procedure, except for using the catalyst: (*R*)- α,α -bis[3,5-bis(trifluoromethyl)phenyl]-2-pyrrolidinemethanol trimethylsilyl ether.

Steady-state fluorescence spectroscopy

Steady-state absorption and emission spectra were recorded on a Hitachi (U-3310) spectrophotometer and an Edinburgh (FS920) fluorimeter, respectively. Both wavelength dependent excitation and emission response of the fluorimeter had been carefully calibrated. To avoid interference from Trp emission, the selected excitation wavelength at 310 nm enables virtually free of absorption by any Trp residues.

Competitive binding experiments were set up with a constant assay concentration of 1 μM (2,7-aza)Trp741-IKK $\beta_{735-745}$ peptide (Scheme 2). Binding curves were fit to a formula describing competitive binding of two different ligands to the same site on a protein[38] using SigmaPlot version 10, and taking into account the respective experimental K_d values. In this study, we chose to hold the tracer probe and inhibitor

concentrations constant while titrating the NEMO rather than the usual approach. This approach has the following advantages. First, the avoidance of possible self-absorption effect and emission interference caused by increasing inhibitor concentrations in the analyzed wavelength region. Second, reduction of potential interference caused by increase in concentration of organic solvent which used to dissolve inhibitor during titration. The disadvantage of our method is that it requires a relatively large amount of purified NEMO protein.

Analysis of the binding mechanism of potential inhibitors

The availability of the X-ray structure of IKK β /NEMO association domain (PDB: 3BRV)[26] allows us to set up a docking protocol to identify new chemical scaffolds able to inhibit the assembly of NEMO/IKK β chains. The 3D structure of the NEMO/IKK β complex shows that two regions in the IKK peptide contribute to binding affinity for NEMO: the linker (732-736) and the NBD (737-742). Two tryptophans in the conserved NBD (Trp741 and Trp739) and a hydrophobic residue from the linker region (F734) constitute the hot spots critical for the NEMO/IKK β complex formation. The structures of the ligands were generated by Discovery Studio 2.1 software and the minimized energy was given by the CHARMM force field. Before docking, the NEMO crystal structure was conducted with the "Clean and

Prepare Protein Program” to model missing loop regions, remove water, add hydrogen, and other procedures as required. The binding sites were created with the coordinates x: 13.6948, y: 1.05125 and z: -1.05798 and a radius of 15 Å. The docking program was performed with the partial flexibility program CDOCKER protocol. Molecular docking results were evaluated based on the CDOCKER energy scores, interaction site, and interaction force types with NEMO.

Supporting information

Protein sequence, describe of competitive binding formula, corresponding structures, synthesis of CP1-CP7, and spectral results.

Corresponding author

049696@mail.fju.edu.tw; chebch@ccu.edu.tw; 034407@mail.fju.edu.tw;

chop@ntu.edu.tw

Author contributions

W.C.C. measured and analyzed the data. P.D.C., T.C.L and J.Y.S. performed the chemical syntheses. T.H.C. and L.J.L. performed protein experiments and analysis. B.C.H., J.F.L., J.S.W., and P.T.C. co-wrote the article. All the authors discussed the results and commented on the manuscript.

Notes

The authors declare no competing financial interests.

Acknowledgments

We acknowledge financial support for this study from the Ministry of Science and Technology (MOST, Taiwan) and thank the instrument center of MOST for analyses of compounds. We also thank the SPR technical support provided by Technology Commons, College of Life Science, National Taiwan University.

Abbreviations used

NF- κ B, nuclear factor- κ B; IKK, I κ B kinase; NEMO, IKK γ ; TNF, tumor necrosis factor; RANKL, receptor activator of NF- κ B ligand.

Reference

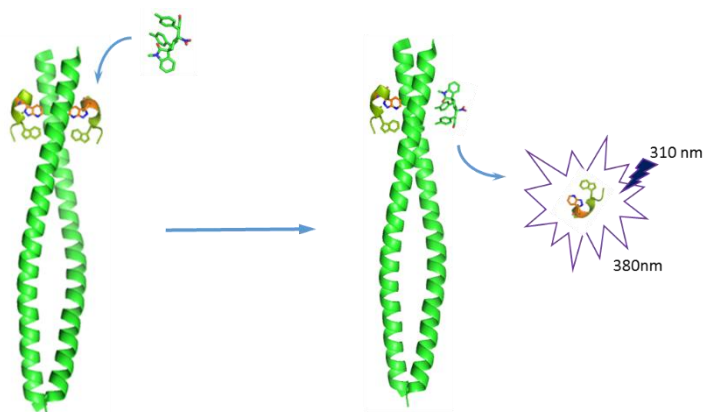
- [1] S. Vallabhapurapu, M. Karin, Regulation and function of NF-kappaB transcription factors in the immune system, *Annu. Rev. Immunol.*, 27 (2009) 693-733.
- [2] J. Napetschnig, H. Wu, Molecular basis of NF-kappaB signaling, *Annu. Rev. Biophys.*, 42 (2013) 443-468.
- [3] M. Karin, M. Delhase, The I kappa B kinase (IKK) and NF-kappa B: key elements of proinflammatory signalling, *Semin. Immunol.*, 12 (2000) 85-98.
- [4] V. Baud, M. Karin, Is NF-kappaB a good target for cancer therapy? Hopes and pitfalls, *Nat. Rev. Drug. Discov.*, 8 (2009) 33-40.
- [5] T.S. Kang, W. Wang, H.J. Zhong, Z.Z. Dong, Q. Huang, S.W. Mok, C.H. Leung, V.K. Wong, D.L. Ma, An anti-prostate cancer benzofuran-conjugated iridium(III) complex as a dual inhibitor of STAT3 and NF-kappaB, *Cancer letters*, 396 (2017) 76-84.

- [6] M. Di Pilato, E. Mejias-Perez, C.O.S. Sorzano, M. Esteban, Distinct Roles of Vaccinia Virus NF-kappaB Inhibitor Proteins A52, B15, and K7 in the Immune Response, *J. Virol.*, 91 (2017).
- [7] J.M. Donovan, M. Zimmer, E. Offman, T. Grant, M. Jirousek, A Novel NF-kappaB Inhibitor, Edasalonexent (CAT-1004), in Development as a Disease-Modifying Treatment for Patients With Duchenne Muscular Dystrophy: Phase 1 Safety, Pharmacokinetics, and Pharmacodynamics in Adult Subjects, *J. Clin. Pharmacol.*, 57 (2017) 627-639.
- [8] K.J. Wu, H.J. Zhong, G. Yang, C. Wu, J.M. Huang, G. Li, D.L. Ma, C.H. Leung, Small Molecule Pin1 Inhibitor Blocking NF-kappaB Signaling in Prostate Cancer Cells, *Chem. Asian J.*, 13 (2018) 275-279.
- [9] X. Deng, X. Zhang, B. Tang, H. Liu, Q. Shen, Y. Liu, L. Lai, Design, Synthesis, and Evaluation of Dihydrobenzo[cd]indole-6-sulfonamide as TNF-alpha Inhibitors, *Front. Chem.*, 6 (2018) 98.
- [10] M. Hinz, C. Scheidereit, The IkappaB kinase complex in NF-kappaB regulation and beyond, *EMBO Rep.*, 15 (2014) 46-61.
- [11] C. Scheidereit, IkappaB kinase complexes: gateways to NF-kappaB activation and transcription, *Oncogene*, 25 (2006) 6685-6705.
- [12] H. Hacker, M. Karin, Regulation and function of IKK and IKK-related kinases, *Sci. STKE*, 2006 (2006) re13.
- [13] K. Clark, S. Nanda, P. Cohen, Molecular control of the NEMO family of ubiquitin-binding proteins, *Nat. Rev. Mol. Cell Biol.*, 14 (2013) 673-685.
- [14] M.S. Hayden, S. Ghosh, NF-kappaB, the first quarter-century: remarkable progress and outstanding questions, *Genes Dev.*, 26 (2012) 203-234.
- [15] G. Cildir, K.C. Low, V. Tergaonkar, Noncanonical NF-kappaB Signaling in Health and Disease, *Trends. Mol. Med.*, 22 (2016) 414-429.
- [16] V.F. Shih, R. Tsui, A. Caldwell, A. Hoffmann, A single NFkappaB system for both canonical and non-canonical signaling, *Cell Res.*, 21 (2011) 86-102.
- [17] Q. Li, I.M. Verma, NF-kappaB regulation in the immune system, *Nat. Rev. Immunol.*, 2 (2002) 725-734.
- [18] E. Dejardin, The alternative NF-kappaB pathway from biochemistry to biology: pitfalls and promises for future drug development, *Biochem. Pharmacol.*, 72 (2006) 1161-1179.
- [19] P.E. Collins, I. Mitxitorena, R.J. Carmody, The Ubiquitination of NF-kappaB Subunits in the Control of Transcription, *Cells*, 5 (2016).
- [20] J.A. DiDonato, F. Mercurio, M. Karin, NF-kappaB and the link between inflammation and cancer, *Immunol. Rev.*, 246 (2012) 379-400.
- [21] M.S. Golden, S.M. Cote, M. Sayeg, B.S. Zerbe, E.A. Villar, D. Beglov, S.L.

- Sazinsky, R.M. Georgiadis, S. Vajda, D. Kozakov, A. Whitty, Comprehensive experimental and computational analysis of binding energy hot spots at the NF-kappaB essential modulator/IKKbeta protein-protein interface, *J. Am. Chem. Soc.*, 135 (2013) 6242-6256.
- [22] M.J. May, F. D'Acquisto, L.A. Madge, J. Glockner, J.S. Pober, S. Ghosh, Selective inhibition of NF-kappaB activation by a peptide that blocks the interaction of NEMO with the IkappaB kinase complex, *Science*, 289 (2000) 1550-1554.
- [23] M.J. May, R.B. Marienfeld, S. Ghosh, Characterization of the Ikappa B-kinase NEMO binding domain, *J. Biol. Chem.*, 277 (2002) 45992-46000.
- [24] E.T. Baima, J.A. Guzova, S. Mathialagan, E.E. Nagiec, M.M. Hardy, L.R. Song, S.L. Bonar, R.A. Weinberg, S.R. Selness, S.S. Woodard, J. Chrencik, W.F. Hood, J.F. Schindler, N. Kishore, G. Mbalaviele, Novel insights into the cellular mechanisms of the anti-inflammatory effects of NF-kappaB essential modulator binding domain peptides, *J. Biol. Chem.*, 285 (2010) 13498-13506.
- [25] A. Gaurier-Hausser, R. Patel, A.S. Baldwin, M.J. May, N.J. Mason, NEMO-binding domain peptide inhibits constitutive NF-kappaB activity and reduces tumor burden in a canine model of relapsed, refractory diffuse large B-cell lymphoma, *Clin. Cancer Res.*, 17 (2011) 4661-4671.
- [26] M. Rushe, L. Silvian, S. Bixler, L.L. Chen, A. Cheung, S. Bowes, H. Cuervo, S. Berkowitz, T. Zheng, K. Guckian, M. Pellegrini, A. Lugovskoy, Structure of a NEMO/IKK-associating domain reveals architecture of the interaction site, *Structure*, 16 (2008) 798-808.
- [27] V. De Filippis, S. De Boni, E. De Dea, D. Dalzoppo, C. Grandi, A. Fontana, Incorporation of the fluorescent amino acid 7-azatryptophan into the core domain 1-47 of hirudin as a probe of hirudin folding and thrombin recognition, *Protein Sci.*, 13 (2004) 1489-1502.
- [28] M. Negreire, F. Gai, S.M. Bellefeuille, J.W. Petrich, Photophysics of a novel optical probe: 7-azaindole, *J. Phys. Chem.*, 95 (1991) 8663-8670.
- [29] J.Y. Shen, W.C. Chao, C. Liu, H.A. Pan, H.C. Yang, C.L. Chen, Y.K. Lan, L.J. Lin, J.S. Wang, J.F. Lu, S. Chun-Wei Chou, K.C. Tang, P.T. Chou, Probing water micro-solvation in proteins by water catalysed proton-transfer tautomerism, *Nat. Commun.*, 4 (2013) 2611.
- [30] W.C. Chao, J.Y. Shen, C.H. Yang, Y.K. Lan, J.H. Yuan, L.J. Lin, H.C. Yang, J.F. Lu, J.S. Wang, K. Wee, Y.H. Chen, P.T. Chou, The In Situ Tryptophan Analogue Probes the Conformational Dynamics in Asparaginase Isozymes, *Biophys. J.*, 110 (2016) 1732-1743.
- [31] W.C. Chao, J.Y. Shen, J.F. Lu, J.S. Wang, H.C. Yang, K. Wee, L.J. Lin, Y.C. Kuo,

- C.H. Yang, S.H. Weng, H.C. Huang, Y.H. Chen, P.T. Chou, Probing water environment of Trp59 in ribonuclease T1: insight of the structure-water network relationship, *J. Phys. Chem. B.*, 119 (2015) 2157-2167.
- [32] A.K. Gupta, M. Bharadwaj, A. Kumar, R. Mehrotra, Spiro-oxindoles as a Promising Class of Small Molecule Inhibitors of p53-MDM2 Interaction Useful in Targeted Cancer Therapy, *Top. Curr. Chem. (Cham)*, 375 (2017) 3.
- [33] H. Kato, A. Kai, T. Kawabata, J.D. Sunderhaus, T.J. McAfoos, J.M. Finefield, Y. Sugimoto, R.M. Williams, S. Tsukamoto, Enantioselective inhibitory abilities of enantiomers of notoamides against RANKL-induced formation of multinuclear osteoclasts, *Bioorg. Med. Chem. Lett.*, 27 (2017) 4975-4978.
- [34] C.F. Chapman, M. Maroncelli, Excited-state tautomerization of 7-azaindole in water, *J. Phys. Chem.*, 96 (1992) 8430-8441.
- [35] Y. Chen, F. Gai, J.W. Petrich, Single-Exponential Fluorescence Decay of the Nonnatural Amino Acid 7-Azatriptophan and the Nonexponential Fluorescence Decay of Tryptophan in Water, *J. Phys. Chem.*, 98 (1994) 2203-2209.
- [36] F. De Falco, C. Di Giovanni, C. Cerchia, D. De Stefano, A. Capuozzo, C. Irace, T. Iuvone, R. Santamaria, R. Carnuccio, A. Lavecchia, Novel non-peptide small molecules preventing IKK β /NEMO association inhibit NF- κ B activation in LPS-stimulated J774 macrophages, *Biochem. Pharmacol.*, 104 (2016) 83-94.
- [37] P.D. Chaudhari, B.-C. Hong, G.-H. Lee, Organocatalytic Enantioselective Michael–Michael–Michael–Aldol Condensation Reactions: Control of Six Stereocenters in a Quadruple-Cascade Asymmetric Synthesis of Polysubstituted Spirocyclic Oxindoles, *Org. Lett.*, 19 (2017) 6112-6115.
- [38] Z.X. Wang, An exact mathematical expression for describing competitive binding of two different ligands to a protein molecule, *FEBS Lett.*, 360 (1995) 111-114.

Table of Contents graphic



ACCEPTED MANUSCRIPT

Highlights

Unnatural amino acid substituted IKK β ₇₃₅₋₇₄₅ peptides to act as fluorescent probes

Sensing polarity, proximal and relayed water molecules around the binding interface

Utilizing a competitive binding platform to screen the binding ability

(-)-PDC-099, a potent agent with ascertained potent to disrupt IKK β -NEMO complex

ACCEPTED MANUSCRIPT